CHAPTER 22

Measuring Surface Tension and Free Surface Energy

22.1 INTRODUCTION

Having introduced the concept of surface tension and free surface energy, we will now turn to methods that allow us to determine these characteristic values. As it turns out, several straightforward and convenient methods allow measuring the surface tension of a liquid. However, measuring the free energy of a surface is inherently more difficult because it is not a property directly accessible to measurement. In most cases, free energies of surfaces are measured *via* the characteristic contact angles that certain liquids will show on these surfaces. Several theoretical models and measurement techniques derived thereby allow determining the free surface energy. In this section we will study the most relevant techniques.

22.2 MEASURING THE SURFACE TENSION OF LIQUIDS

The surface tension of a liquid can be obtained experimentally by using a *tensiometer*. Several tensiometers are in common use today.

22.2.1 du Noüy Ring

A very common tensiometric method is based on the technique first described by French physicist Pierre du Noüy in 1925 [1]. It uses a thin platinum ring that is slowly lifted off the surface of a liquid. The force required can be used to directly calculate the surface tension according to

$$\begin{aligned} F_{\text{measured}} &= \gamma_{\text{liquid}}\, l_c \\ &= \gamma_{\text{liquid}}\, 2\pi \left(r_{\text{inner}} + r_{\text{outer}}\right) \end{aligned}$$

Remember that if the force has to be calculated, we always have to use the circumference l_c as the relevant length to be multiplied with the surface tension. The values measured using du Noüy rings usually have to be corrected to compensate for the shape of the liquid meniscus forming at the boundary of the ring that change the direction of action of the surface tension forces. These correction factors depend heavily on the shape of the rings used.

22.2.2 Wilhelmy Plate Method

Another method for measuring the surface tension is the *Wilhelmy plate method*, which was first used by the German chemist Ludwig Wilhelmy in 1863 [2]. In this setup a *Wilhelmy plate* is either immersed or retracted from a liquid with unknown surface tension (see Fig. 22.1a). In the immersion case, the surface will form an advancing contact angle with the liquid. In the retraction case, the surface will form a receding contact angle with the liquid. In both cases the surface tension will pull the plate into the liquid. The plate is held by an external force F_{external} that is adjusted such that the plate does not move. The balance of forces on the plate then is

$$F_{\text{external}} + F_{\text{buoyancy}} - F_{\gamma,\text{gas/liquid}} - F_{\gamma,\text{liquid/solid}} - F_{\text{gravity}} = 0 \qquad \text{(Eq. 22.1)}$$

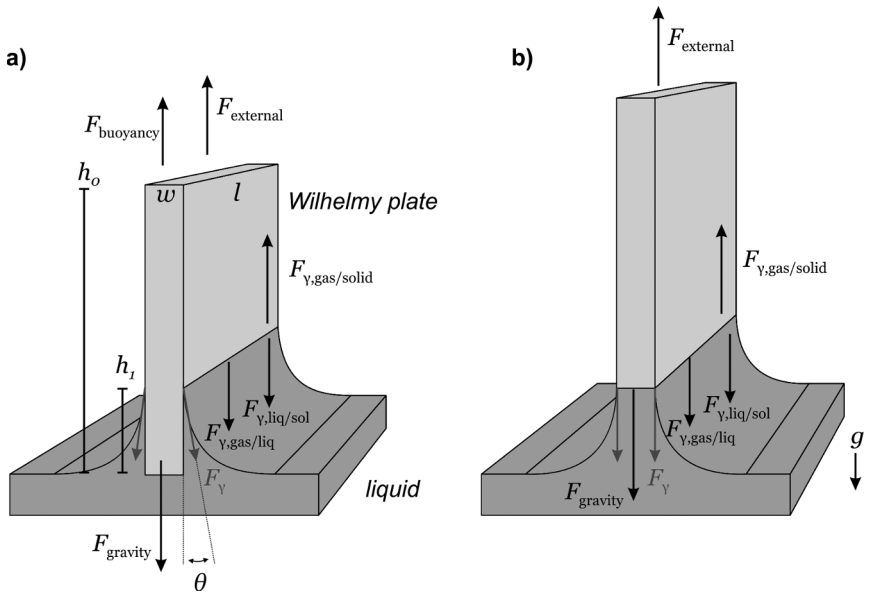

Fig. 22.1 *Wilhelmy plate method for measuring the surface tension of a liquid. a) A Wilhelmy plate is slowly pulled out or inserted into a liquid. The free surface energy will give rise to the characteristic receding or advancing contact angles. An external force $F_{external}$ is applied to the plate in order to keep it stationary thus compensating the surface tension. b) Shortly before the plate is completely pulled off the surface, $F_{external}$ is at a maximum value.*

with

$$
\begin{aligned}
F_{\text{buoyancy}} &= \rho\, l\, w\, h_1\, g \\
F_{\gamma,\text{gas/liquid}} &= 2\,(l+w)\,\gamma\,\cos\Theta \\
F_{\gamma,\text{liquid/solid}} &\approx 0 \text{ or constant} \\
F_{\text{gravity}} &= \rho\, l\, w\, h_0\, g
\end{aligned}
$$

Shortly before the plate detaches completely from the surface, F_{external} reaches its maximum values (see Fig. 22.1b). At this location no buoyancy forces are acting, and $\Theta = 0°$. Therefore Eq. 22.1 simplifies to

$$
\begin{aligned}
F_{\text{external}} - F_{\gamma,\text{gas/liquid}} - F_{\text{gravity}} &= 0 \\
F_{\text{external}} - 2\,(l+w)\,\gamma - \rho\, l\, w\, h_0\, g &= 0 \\
\gamma &= \frac{F_{\text{external}} - \rho\, l\, w\, h_0\, g}{2\,(l+w)}
\end{aligned}
$$

If F_{external} can be determined at sufficient precision, all terms of Eq. 22.1 can be calculated except $F_{\gamma,\text{liquid/solid}}$. For very small contact angles, this term is almost 0 (see Eq. 20.4). This condition is effected by using platinum as material for the Wilhelmy plate which will (when sufficiently clean) will form an almost zero contact angle with most liquids because of its high free surface energy (see Tab. 20.1).

There are several modifications of the Wilhelmy plate method, with the most common one using a platinum rod instead of a plate. This allows measurement in smaller vessels and is thus suitable for applications where only minor amounts of the liquid can be provided. Compared to the du Noüy measurements, values obtained from the Wilhelmy plate method do not have to be compensated because there is shape-dependent meniscus formation at the plate surface.

22.2.3 Drop-Weight Method

The surface tension can also be derived by observing the characteristic deformation of a pendant drop at the end of a capillary (see Fig. 22.2). In these equations, surface tension balances gravity forces

$$
\begin{aligned}
F_\gamma &= F_{\text{gravity}} \\
\gamma\,\pi\, d\,\sin\Theta &= m\, g
\end{aligned}
\qquad \text{(Eq. 22.2)}
$$

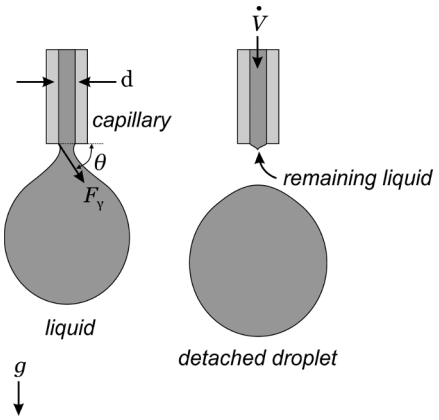

Fig. 22.2 *The drop-weight method measures the weight of droplets falling off a capillary tip. It is important to note that not the entire liquid will fall off the tip; this must be corrected in the theoretical models.*

Eq. 22.2 is referred to as *Tate's law* first described by Tate in 1864 [3]. If more and more liquid is pushed into the droplet *via* the capillary, the total mass of the droplet will increase. This increase is balanced by an increase in the contact angle, as all other parameters on the left-hand side of Eq. 22.2 are constant. The droplet will fall from the capillary once the contact angle reaches 90°, in which case

$$\gamma = \frac{m\,g}{\pi\,d} \qquad \text{(Eq. 22.3)}$$

Therefore the surface tension can be measured (in theory) by weighting the mass of droplets that fall off the capillary. If d cannot be determined, the surface tension can be measured in a differential manner by using a reference liquid with known surface tension (usually pure water or a suitable solvent). The same ratio $\frac{\eta}{m}$ will be constant for both liquids; therefore the surface tension to be determined can be obtained from the value of the reference liquid.

This method is referred to as the *drop-weight method*. The respective instrument for performing drop-weight-based surface tension determinations is referred to as a *stalagmometer*. In practical experiments, a larger portion of the droplet will remain attached to the capillary. Therefore a correction factor ξ is applied to Eq. 22.3 resulting in

$$\gamma = \xi\,\frac{m\,g}{\pi\,d} \qquad \text{(Eq. 22.4)}$$

The correction factor ξ is a function only of the capillary diameter d and the droplet mass m (actually of the droplet volume V to be precise) but not of the surface tension. This allows applying Eq. 22.4 once the droplet mass has been determined by looking up the correction factor in the reference literature.

22.2.4 Pendant Drop Analysis

22.2.4.1 Introduction

A very common method of deriving the surface tension is by inspection of the characteristic shape of a pendant droplet. These methods are generally used for *pendant drop analysis*. As we will see in section 24, the fluid mechanics of the pendant and sessile droplet are surprisingly complex. The underlying equation turns out to be a inhomogeneous ODE given by Eq. 24.5. Usually solutions to this equation must be derived numerically, as we will see. Section 24.2 describes several modifications to this original equation to make it numerically more accessible. Drop shapes are usually calculated for different values of the density ρ and the surface tension γ and are compared to the drop contour recorded, *e.g.*, using a charge-coupled device (CCD) camera. The measured and calculated contour are compared using, *e.g.*, a least-square algorithm to determine the closest matching geometry and thus derive the surface tension. Usually, the density of the fluid has to be determined prior to measuring the surface tension in order to find a single drop contour. If both density and surface tension are unknown there may be more than one solution to the drop profile, as both independent variables are used as product in Eq. 24.5.

22.2.4.2 d_e/d_s Method

The d_e/d_s method records only two lengths of a pendant droplet (see Fig. 22.3). The first diameter d_e is the maximum diameter of the droplet. The second diameter d_s is the diameter at the location that is exactly the distance d_e from the lowest point of the droplet. For this method, a shape factor S is introduced and is defined as

$$S = \frac{d_s}{d_e}$$

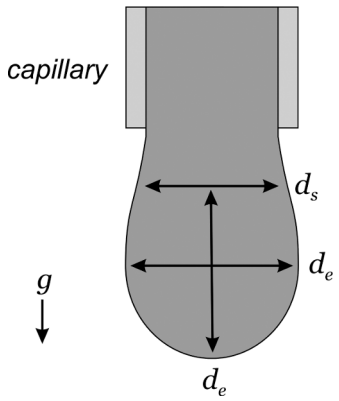

Fig. 22.3 *Determination of the surface tension using the d_e/d_s.*

which is primarily dependent on the shape of the drop. The second equation is based on Eq. 24.5; it uses the first term on the right-hand side, which is first made dimensionless by multiplying it by $r_{\theta,\max}$. Next z is made dimensionless by dividing it by $r_{\theta,\max}$, in which case the prefactor must be multiplied by $r_{\theta,\max}$ again. The resulting factor β thus becomes

$$\beta = \frac{\Delta\rho\, g\, r_{\theta,\max}^2}{\gamma} \qquad \text{(Eq. 22.5)}$$

As one can see, β essentially is the Eötvös or Bond number (see section 9.9.9). Now Eq. 22.5 can be solved for the surface tension to result in

$$\begin{aligned}\gamma &= \frac{\Delta\rho\, g\, r_{\theta,\max}^2}{\beta} \\ &= \frac{\Delta\rho\, g\, d_e^2}{\beta\left(\frac{d_e}{r_{\theta,\max}}\right)^2} = \frac{\Delta\rho\, g\, d_e^2}{H}\end{aligned} \qquad \text{(Eq. 22.6)}$$

where we introduced the factor H as

$$H = \beta\left(\frac{d_e}{r_{\theta,\max}}\right)^2 = f(S)$$

which is a function of the shape factor. If the shape factor can be determined sufficiently precise, the surface tension can also be calculated sufficiently precise. In many cases, this simplified method is sufficiently exact to yield useful values for the surface tension. Most modern computer vision-based instruments for pendant drop analysis are based on this algorithm.

22.2.5 Maximum Bubble Pressure Method

A very easy and convenient method for measuring the surface tension is referred to as the *maximum bubble pressure method*. In this method a capillary is immersed into the liquid to be measured, and a gas bubble is created inside the liquid using gas with controllable pressure (see Fig. 22.4). As the pressure increases, the size

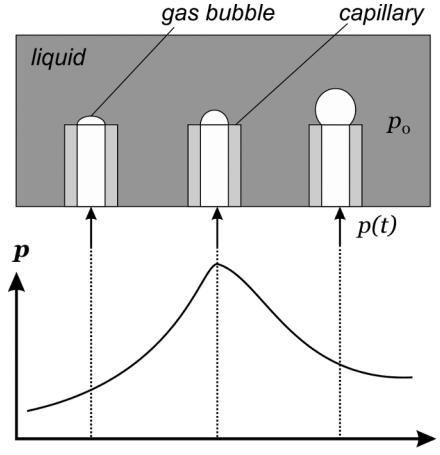

Fig. 22.4 *Maximum bubble pressure method for measuring the surface tension. A gas bubble is expanded in a fluid by applying gas at a controllable pressure. If the radius of the bubble matches the radius of the capillary, the pressure is at a maximum. Expanding the bubble further will reduce the pressure and lead to the detachment of the bubble.*

of the bubble increases until its diameter is identical to the diameter of the capillary (hemispherical bubble). In this case the Young-Laplace equation allows determining the surface tension using

$$\begin{aligned} p_{\max} - p_0 &= \gamma \left(\frac{1}{r_1} + \frac{1}{r_2} \right) \\ &= \gamma \frac{2}{r_{\text{capillary}}} \\ \gamma &= \frac{(p_{\max} - p_0)\, r_{\text{capillary}}}{2} \end{aligned}$$

The maximum bubble pressure method is often used to measure the dynamic surface tension, as it allows measuring the development of the surface tension at a newly created interface. For example, in a surfactant solution, the molecules will (over time) assemble at the gas/liquid interface and change the surface tension. The changing surface tension can be measured conveniently at the changes in bubble size over time if the pressure is kept constant.

22.2.6 Spinning-Drop Method

Another method for measuring the surface tension is the *spinning-drop method* originally developed and described by Vonnegut [4]. This method uses a droplet of a liquid or a gas that is suspended in a second immersion fluid. If the whole setup is rotated at high speeds, the drop will deform under the action of the centrifugal force (see Fig. 22.5). The deformation of the droplet allows deriving the surface tension.

The method is very precise, and surface tensions down to several $10^{-6}\,\text{mN}\,\text{m}^{-1}$ can be measured accurately. In addition, this is one of the few methods that allows measuring the interfacial surface tension between two liquids, one of which forms the droplet with the other one forming the surrounding liquid.

The elongated shape of the spinning drop can be well approximated as a cylinder with two hemispherical caps (see Fig. 22.6a). As the drop changes its surface area, two energy terms are involved: the change of energy because of the action of the surface tension and the change of energy because of the action of the centrifugal forces.

We will consider a drop being rotated at the angular velocity ω resulting in a drop of length L and diameter R.

Energy Contribution of the Surface Tension. The change of energy because of the surface tension is given by

$$\begin{aligned} dE_{\text{surface tension}} &= \gamma\, dA \\ &= \gamma\, (dA_{\text{sphere}} + dA_{\text{cylinder}}) \\ &= \gamma\, (8\,\pi\, r\, dr + 2\,\pi\, L\, dr) \end{aligned} \qquad \text{(Eq. 22.7)}$$

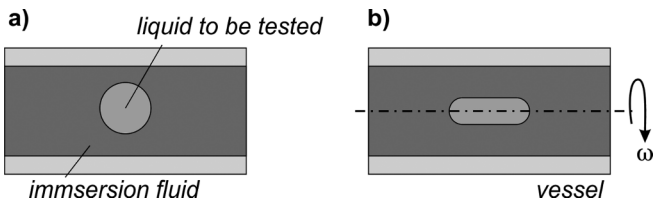

Fig. 22.5 *The concept of the spinning drop method. a) A liquid drop is immersed in a second liquid. b) Upon rotation the drop is elongated. The elongation of the drop allows deriving the interfacial surface tension.*

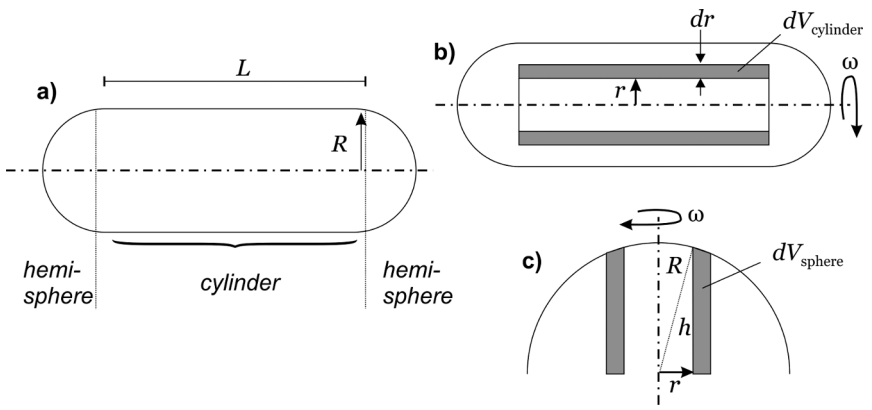

Fig. 22.6 *Model for the derivation of the spinning drop mechanics. a) The drop is approximated as a cylinder with hemispherical caps. b) Infinitesimal mass $dV_{cylinder}$ at the cylinder section of the spinning drop. c) Infinitesimal mass dV_{sphere} at the hemispherical section of the spinning drop.*

The area consists of the surface area of the cylinder and of the two hemispheres (a complete sphere in total). We have therefore used Eq. 3.105 and Eq. 3.107 for the infinitesimal surface change of a cylinder and a sphere, respectively. Integration of Eq. 22.7 yields

$$\begin{aligned}\int dE_{\text{surface tension}} &= \int_0^R \gamma\ (8\,\pi\,r\,dr + 2\,\pi\,L\,dr)\\ E_{\text{surface tension}} &= \gamma\ \left(4\,\pi\,R^2 + 2\,\pi\,R\,L\right)\end{aligned} \qquad \text{(Eq. 22.8)}$$

As L changes, it is better to express it as a function of the drop volume V, which obviously remains constant. Therefore

$$\begin{aligned}V_{\text{drop}} &= V_{\text{sphere}} + V_{\text{cylinder}}\\ &= \frac{4}{3}\,\pi\,R^3 + \pi\,R^2\,L\\ L &= \frac{V_{\text{drop}} - \frac{4}{3}\,\pi\,R^3}{\pi\,R^2}\\ &= \frac{V_{\text{drop}}}{\pi\,R^2} - \frac{4}{3}\,R\end{aligned} \qquad \text{(Eq. 22.9)}$$

which yields after substitution in Eq. 22.8

$$\begin{aligned}E_{\text{surface tension}} &= \gamma\ \left(4\,\pi\,R^2 + 2\,\pi\,R\ \left(\frac{V_{\text{drop}}}{\pi\,R^2} - \frac{4}{3}\,R\right)\right)\\ &= \gamma\,\pi\ \left(\frac{2\,V_{\text{drop}}}{\pi\,R} + \frac{4}{3}\,R^2\right)\end{aligned} \qquad \text{(Eq. 22.10)}$$

Here the surface tension value used is the interfacial surface tension between the liquid of the drop and the surrounding immersion liquid.

Energy Contribution of the Rotation. The energy that is due to the rotation is given by

$$dE_{\text{rotation}} = \frac{1}{2}\,\Delta\rho\,\omega^2\,r^2\,dV \qquad \text{(Eq. 22.11)}$$

where we used the differences in density of the two liquids $\Delta\rho$. The change of volume dV can be expressed as

$$\begin{aligned}dV &= dV_{\text{cylinder}} + dV_{\text{sphere}}\\ &= 2\,\pi\,L\,r\,dr + dV_{\text{sphere}}\end{aligned} \qquad \text{(Eq. 22.12)}$$

where we used Eq. 3.106 for the infinitesimal change in volume for a cylinder (see Fig. 22.6b). Determining dV_{sphere} is a bit more complicated because we need to consider the hemisphere as segments weighted with their respective distance to the center axis (see Fig. 22.6c). This effectively splits the hemispheres into individual rings with different heights h that can be determined geometrically as

$$h = \sqrt{R^2 - r^2}$$

dV_{sphere} can then be expressed as

$$\begin{aligned}dV_{\text{sphere}} &= h\,dA_{\text{circle}}\\ &= \sqrt{R^2 - r^2}\,2\,\pi\,r\,dr\end{aligned} \qquad \text{(Eq. 22.13)}$$

where we used Eq. 3.104 for expressing the infinitesimal change of the circle area. Note that we need to multiply this equation by two in order to account for both hemispheres. Inserting Eq. 22.12 and Eq. 22.13 into Eq. 22.11 yields

$$\begin{aligned}dE_{\text{rotation}} &= \frac{1}{2}\,\Delta\rho\,\omega^2\,r^2\ \left(2\,\pi\,L\,r\,dr + 2\,\sqrt{R^2 - r^2}\,2\,\pi\,r\,dr\right)\\ dE_{\text{rotation}} &= \Delta\rho\,\omega^2\,\pi\ \left(L\,r^3 + \sqrt{R^2 - r^2}\,r^3\right)\,dr\\ \int dE_{\text{rotation}} &= \Delta\rho\,\omega^2\,\pi\ \int_0^R \left(L\,r^3 + \sqrt{R^2 - r^2}\,r^3\right)\,dr\\ E_{\text{rotation}} &= \Delta\rho\,\omega^2\,\pi\ \left(\frac{L}{4}R^4 + \frac{4}{15}R^5\right)\end{aligned} \qquad \text{(Eq. 22.14)}$$

In the last step we replace L using Eq. 22.9 resulting in

$$\begin{aligned} E_{\text{rotation}} &= \Delta\rho\,\omega^2\,\pi\,\left(\frac{1}{4}\,\left(\frac{V_{\text{drop}}}{\pi}\,R^2 - \frac{4}{3}\,R^5\right) + \frac{4}{15}R^5\right) \\ &= \Delta\rho\,\omega^2\,\pi\,\left(\frac{1}{4}\,\frac{V_{\text{drop}}}{\pi}\,R^2 - \frac{1}{15}\,R^5\right) \end{aligned} \qquad \text{(Eq. 22.15)}$$

Energy Minimum. In order for the drop to achieve a stable form, the energy contributions upon change of the droplet's shape must be minimized. Therefore

$$\frac{d}{dR}\left(E_{\text{surface tension}} + E_{\text{rotation}}\right) \stackrel{!}{=} 0 \qquad \text{(Eq. 22.16)}$$

Inserting Eq. 22.10 and Eq. 22.15 into Eq. 22.15 yields

$$0 \stackrel{!}{=} \frac{d}{dR}\left(\gamma\,\pi\,\left(\frac{2\,V_{\text{drop}}}{\pi\,R} + \frac{4}{3}\,R^2\right) + \Delta\rho\,\omega^2\,\pi\,\left(\frac{1}{4}\,\frac{V_{\text{drop}}}{\pi}\,R^2 - \frac{1}{15}\,R^5\right)\right) \qquad \text{(Eq. 22.17)}$$

$$0 \stackrel{!}{=} \gamma\,\pi\,\left(-\frac{2\,V_{\text{drop}}}{\pi\,R^2} + \frac{8}{3}\,R\right) + \Delta\rho\,\omega^2\,\pi\,\left(\frac{1}{2}\,\frac{V_{\text{drop}}}{\pi}\,R - \frac{1}{3}\,R^4\right)$$

$$0 \stackrel{!}{=} -\,\gamma\,\pi\,2\,\left(\frac{V_{\text{drop}}}{\pi\,R^2} - \frac{4}{3}\,R\right) + \Delta\rho\,\omega^2\,\pi\,R^3\,\left(\frac{1}{2}\,\frac{V_{\text{drop}}}{\pi\,R^2} - \frac{1}{3}\,R\right)$$

$$0 \stackrel{!}{=} -\,\gamma\,\pi\,2\,L + \Delta\rho\,\omega^2\,\frac{1}{2}\,\pi\,R^3\,\left(\frac{V_{\text{drop}}}{\pi\,R^2} - \frac{4}{3}\,R + \frac{2}{3}\,R\right)$$

$$0 \stackrel{!}{=} -\,\gamma\,\pi\,2\,L + \Delta\rho\,\omega^2\,\frac{1}{2}\,\pi\,R^3\,\left(L + \frac{2}{3}\,R\right)$$

$$\gamma = \frac{1}{2\,L}\Delta\rho\,\omega^2\,\frac{1}{2}\,R^3\,\left(L + \frac{2}{3}\,R\right)$$

$$\gamma = \frac{\Delta\rho\,\omega^2\,R^3}{2}\,\left(\frac{1}{2} + \frac{1}{3}\,\frac{R}{L}\right) \qquad \text{(Eq. 22.18)}$$

Eq. 22.18 allows determining the surface tension simply by measuring R and L of the rotating drop.

Very Long Drops. At higher rotation speeds, the droplet formed is merely a cylinder and $\frac{R}{L} \to \infty$, in which case Eq. 22.18 simplifies to

$$\gamma = \frac{\Delta\rho\,\omega^2\,R^3}{4} \qquad \text{(Eq. 22.19)}$$

Here it is only required to measure the radius of the droplet formed in order to determine the surface tension.

A Comment to the Usage of *L*. You may have noticed that we did not replace L when performing the integrations for $E_{\text{surface tension}}$ (see Eq. 22.8) and E_{rotation} (see Eq. 22.14). However, we inserted L prior to differentiating when determining the energy minimum (see Eq. 22.17). This is due to the fact that we developed the energy contributions such that they resulted in a constant L, as we were increasing only the diameter of the cylinder and the radius of the hemispheres. However, during the determination of the energy minimum, both L and R will change in order to keep the volume V_{drop} constant. This is why we cannot treat L as a constant when deriving Eq. 22.17.

22.2.7 Measurement by Capillarity

Surface tensions can also be measured by capillarity (see section 21) and can be derived directly from the capillary rise in a tube. For this the capillary height h_c must be determined as well as the contact angle Θ. By using Eq. 21.3, the surface tension can then be calculated.

22.3 MEASURING THE FREE SURFACE ENERGY

As stated, determining the free surface energies of solid surfaces is inherently more difficult than measuring the free surface energy, *i.e.*, the surface tension of a liquid. For surfaces, the measurement is usually accomplished indirectly by depositing different liquids on the surface and measurement of the resulting contact angles. Depending on the nature of the liquid, it is possible to deduce the imbalanced intermolecular forces in the surface.

The Young's equation (see Eq. 20.4) is the basis of these techniques. In order to find $\gamma_{\text{gas/solid}}$, which essentially is the free surface energy of the surface in contact with the ambiance, we need $\gamma_{\text{gas/liquid}}$ (which is the surface tension that can be measured) and $\gamma_{\text{liquid/solid}}$ (which we cannot measure).

We therefore have to approximate $\gamma_{\text{liquid/solid}}$ by a suitable model. We will begin by considering the potential interaction forces between the liquid and the solid. The most important ones are

- polar interaction γ^{p} resulting from permanent dipole interaction
- disperse interaction γ^{d} resulting primarily from London dispersion forces
- hydrogen interaction γ^{h} resulting from hydrogen bonding
- metal bonding γ^{mb} resulting from the action of inter-surface metal bonds
- acid/base interaction γ^{ab} resulting from the action of proton exchange

The interaction of a liquid and a solid will take place only if both components are able to interact by the given bond. An unpolar liquid has very low polar interaction and thus will not interact strongly with a polar surface. As we will see, this is an important detail because it allows us to actually determine the individual components in Eq. 22.20.

Essentially, the total interaction of the liquid and the solid can be described by the sum of these contributions. Several models are used in order to relate these interactions to $\gamma_{\text{liquid/solid}}$. The most important concept is based on solubility dynamics. It is explained in detail in [5] and states that

$$\gamma_{\text{liquid/solid}} = \gamma_{\text{gas/liquid}} + \gamma_{\text{gas/solid}} - \sum_{i=\{\text{p,d,h,mb,ab}\}} 2\sqrt{\gamma^{\text{i}}_{\text{gas/liquid}}\,\gamma^{\text{i}}_{\text{gas/solid}}} \qquad \text{(Eq. 22.20)}$$

We can now rewrite Eq. 20.3 using Eq. 22.20 as

$$\begin{aligned}\cos\Theta\,\gamma_{\text{gas/liquid}} &= \gamma_{\text{gas/solid}} - \gamma_{\text{gas/liquid}} - \gamma_{\text{gas/solid}} + \sum_{i=\{\text{p,d,h,mb,ab}\}} 2\sqrt{\gamma^{\text{i}}_{\text{gas/liquid}}\,\gamma^{\text{i}}_{\text{gas/solid}}} \\ (\cos\Theta + 1)\,\gamma_{\text{gas/liquid}} &= \sum_{i=\{\text{p,d,h,mb,ab}\}} 2\sqrt{\gamma^{\text{i}}_{\text{gas/liquid}}\,\gamma^{\text{i}}_{\text{gas/solid}}} \qquad \text{(Eq. 22.21)}\end{aligned}$$

Several commonly used methods are found in the literature that basically differ only in the interaction contributions they take into account. For all of these experiments, standard reference liquids are used for which the respective contribution $\gamma^{\text{i}}_{\text{gas/liquid}}$ are known. Therefore, for each additional contribution taken into account, one additional measurement must be performed in order to calculate the respective unknown contribution of the surface $\gamma^{\text{i}}_{\text{gas/liquid}}$. Once all contributions have been determined, the values can be calculated as

$$\gamma_{\text{gas/solid}} = \sum_{i=\{\text{p,d,h,mb,ab}\}} \gamma^{\text{i}}_{\text{gas/solid}}$$

In the following sections, we will briefly discuss the most commonly used models and approaches.

22.3.1 Fowkes Model

American physicist Frederik Fowkes who first suggested the concept laid out in Eq. 22.20 in 1962 [6] assumed the interaction to be primarily dispersive and polar. Therefore Eq. 22.21 is rewritten as

$$(\cos\Theta + 1)\,\gamma_{\text{gas/liquid}} = 2\sqrt{\gamma^{\text{d}}_{\text{gas/liquid}}\,\gamma^{\text{d}}_{\text{gas/liquid}}} + 2\sqrt{\gamma^{\text{p}}_{\text{gas/liquid}}\,\gamma^{\text{p}}_{\text{gas/solid}}} \qquad \text{(Eq. 22.22)}$$

Experimentally, the dispersive component is first determined by a measurement using diiodomethane, which has no polar contribution. Therefore Eq. 22.22 can be used to solve for $\gamma^{\text{d}}_{\text{gas/solid}}$. In the next step, water is used in order to solve Eq. 22.22 for $\gamma^{\text{p}}_{\text{gas/solid}}$. As $\gamma^{\text{d}}_{\text{gas/solid}}$ is known, the equation is easy to solve.

Tab. 22.1 lists the liquids most commonly used for measuring the free surface energy. It lists the contributions to the surface tension of the test liquids as the polar and the disperse contribution. In the following, we will provide an example using the Fowkes method for the determination of the free surface energy of polystyrene.

Tab. 22.1 *Liquids commonly used for determining free surface energies [7–9]. All values given are in* $mN\,m^{-1}$

Substance	Surf. tens.	Fowkes		Extended Fowkes			OCG		
	$\gamma_{gas/liquid}$	$\gamma^{d}_{gas/liquid}$	$\gamma^{p}_{gas/liquid}$	$\gamma^{d}_{gas/liquid}$	$\gamma^{p}_{gas/liquid}$	$\gamma^{h}_{gas/liquid}$	$\gamma^{LW}_{gas/liquid}$	$\gamma^{+}_{gas/liquid}$	$\gamma^{-}_{gas/liquid}$
water	72.80	21.80	51	29.10	1.30	42.40	21.80	25.50	25.50
diiodomethane	50.80	0							
glycerol	64	34	30	37.40	0.20	25.80	34	3.92	57.40
formamide	58.20	39	19	35.10	1.60	21.50	39	2.28	39.60
ethylene glycol	47.70	30.90	16.80	30.10	0	17.60	29	3	30.10
1-octanol	27.50	27.50	0				27.50	0	3.97
n-octane	21.62	21.62	0	21.62	0	0	21.62	0	0
chloroform	27.15	27.15	0				27.15	1.50	0

Determining the Free Surface Energy of Polystyrene Using the Fowkes Method. Contact angle measurements are carried out on a sheet of freshly cut polystyrene. Using diiodomethane, we measure the following contact angles: 21°, 16°, 15°, and 11°. From these values, the mean contact angle of 15.75° is calculated. The free surface energy, *i.e.*, the surface tension of diiodomethane, is found to be $50.8\,\mathrm{J\,m^{-2}}$ with $\gamma^{\mathrm{d}}_{\mathrm{gas/liquid}} = 50.8\,\mathrm{mN\,m^{-1}}$ and $\gamma^{\mathrm{p}}_{\mathrm{gas/liquid}} = 0\,\mathrm{mN\,m^{-1}}$ (purely disperse) as shown in Tab. 22.1. Using Eq. 22.22, we obtain

$$\begin{aligned}(\cos(15.75°)+1)\ 50.8\,\mathrm{mN\,m^{-1}} &= 2\sqrt{50.8\,\mathrm{mN\,m^{-1}}\,\gamma^{\mathrm{d}}_{\mathrm{gas/solid}}} + 2\sqrt{0\,\mathrm{mN\,m^{-1}}\,\gamma^{\mathrm{p}}_{\mathrm{gas/solid}}}\\ &= 2\sqrt{50.8\,\mathrm{mN\,m^{-1}}\,\gamma^{\mathrm{d}}_{\mathrm{gas/solid}}}\\ \gamma^{\mathrm{d}}_{\mathrm{gas/solid}} &= 9.91\times10^{-6}\,\mathrm{mN\,m^{-1}}\end{aligned}$$

In a similar experiment using water as test liquid, the following contact angles were measured: 71°, 68°, 72°, and 71°. From these values, the mean contact angle is 70.5°. As shown in Tab. 22.1, the following values for water are obtained: $72.80\,\mathrm{mN\,m^{-1}}$ with $\gamma^{\mathrm{d}}_{\mathrm{gas/liquid}} = 21.8\,\mathrm{mN\,m^{-1}}$ and $\gamma^{\mathrm{p}}_{\mathrm{gas/liquid}} = 51\,\mathrm{mN\,m^{-1}}$ (mixed but predominantly polar). Using Eq. 22.22, we obtain

$$\begin{aligned}(\cos(70.5°)+1)\ 72.80\,\mathrm{mN\,m^{-1}} &= 2\sqrt{21.8\,\mathrm{J\,m^{-2}}\,9.91\times10^{-6}\,\mathrm{mN\,m^{-1}}} + 2\sqrt{51\,\mathrm{J\,m^{-2}}\,\gamma^{\mathrm{p}}_{\mathrm{gas/solid}}}\\ \gamma^{\mathrm{p}}_{\mathrm{gas/solid}} &= 36.44\,\mathrm{mN\,m^{-1}}\end{aligned}$$

From these two experiments, the total free surface energy of polystyrene can be calculated to be $\gamma_{\mathrm{gas/solid}} = 36.44\,\mathrm{mN\,m^{-1}}$, which is very close to the values reported (see Tab. 22.2).

We can already observe an interesting fact about polystyrene: the polymer contributes almost no dispersal forces to the free surface energy. The value is dominated by the contribution of the polar forces. This is one of the reasons why polystyrene is such an interesting material, *e.g.*, for cell culture experiments for which polystyrene is the *de facto* gold standard.

22.3.2 Extended Fowkes Model

Fowkes later extended his original approach taking into account hydrogen interaction in addition to dispersive and polar interaction [10]. Because we have three unknown contributions, a minimum of three measurements must be performed. Tab. 22.1 lists the values for the hydrogen interaction for commonly used test liquids.

22.3.3 Owens, Wendt, Rabel, and Kaelble (OWRK) Model

The models proposed by Owens and Wendt [11] as well by Rabel [12] and Kaelble [13] use the original Fowkes model but change the way the experimental results are read from the data. Essentially, by dividing Eq. 22.22 by $2\sqrt{\gamma^{\mathrm{d}}_{\mathrm{gas/liquid}}}$, the following equation is obtained:

$$\frac{(\cos\Theta+1)\,\gamma_{\mathrm{gas/liquid}}}{2\sqrt{\gamma^{\mathrm{d}}_{\mathrm{gas/liquid}}}} = \sqrt{\gamma^{\mathrm{d}}_{\mathrm{gas/solid}}} + \frac{\sqrt{\gamma^{\mathrm{p}}_{\mathrm{gas/liquid}}}}{\sqrt{\gamma^{\mathrm{d}}_{\mathrm{gas/liquid}}}}\sqrt{\gamma^{\mathrm{p}}_{\mathrm{gas/solid}}}$$

Please note that this is a function of type $y = mx + c$ with $x = \sqrt{\gamma^{\mathrm{p}}_{\mathrm{gas/liquid}}}$ and $c = \sqrt{\gamma^{\mathrm{d}}_{\mathrm{gas/solid}}}$. For different liquids tested, for which we know both $\gamma^{\mathrm{p}}_{\mathrm{gas/liquid}}$ and $\gamma^{\mathrm{d}}_{\mathrm{gas/liquid}}$, we will obtain a linear function with the slope $\sqrt{\gamma^{\mathrm{p}}_{\mathrm{gas/solid}}}$ from which we can directly obtain $\gamma^{\mathrm{p}}_{\mathrm{gas/solid}}$. Extrapolating this line to the intersection with the vertical axis will give us $\gamma^{\mathrm{d}}_{\mathrm{gas/solid}}$.

22.3.4 Wu Model

Wu suggested a different method for calculating the contribution of the polar and the disperse forces [14, 15]. According to Wu, Eq. 22.22 should be expressed as

$$(\cos\Theta+1)\,\gamma_{\mathrm{gas/liquid}} = 4\left(\frac{\gamma^{\mathrm{d}}_{\mathrm{gas/liquid}}\,\gamma^{\mathrm{d}}_{\mathrm{gas/solid}}}{\gamma^{\mathrm{d}}_{\mathrm{gas/liquid}}+\gamma^{\mathrm{d}}_{\mathrm{gas/solid}}} + \frac{\gamma^{\mathrm{p}}_{\mathrm{gas/liquid}}\,\gamma^{\mathrm{p}}_{\mathrm{gas/solid}}}{\gamma^{\mathrm{p}}_{\mathrm{gas/liquid}}+\gamma^{\mathrm{p}}_{\mathrm{gas/solid}}}\right)$$

In this approximation the contributions are included by means of their geometric mean values. The experimental procedure is identical to the Fowkes method.

22.3.5 van Oss, Chaudhury, and Good (OCG) Model

Van Oss, Chaudhury, and Good reformulate the original Fowkes model and detail the nature of the polar interaction [16]. The polar interaction is associated with the action of donor acceptor pairs with two terms that reflect the concentration of donors in the liquid and acceptors in the surface and *v.v.* Furthermore, the dispersive contributions are corrected to account for Debye and Keesom interaction in addition to London dispersion. The resulting contribution is referred to as the *Lifshitz/Van der Waals* contribution $\gamma^{\mathrm{LW}}_{\mathrm{gas/liquid}}$. Eq. 22.22 is thus expanded to

$$(\cos\Theta + 1)\,\gamma_{\mathrm{gas/liquid}} = 2\sqrt{\gamma^{\mathrm{LW}}_{\mathrm{gas/liquid}}\,\gamma^{\mathrm{LW}}_{\mathrm{gas/liquid}}} + 2\sqrt{\gamma^{+}_{\mathrm{gas/liquid}}\,\gamma^{-}_{\mathrm{gas/solid}}} + 2\sqrt{\gamma^{-}_{\mathrm{gas/liquid}}\,\gamma^{+}_{\mathrm{gas/solid}}}$$

Occasionally, a reduced model is also used in which the dispersive contributions are unchanged compared to the Fowkes model. This model is then often referred to as *van Oss and Good model*. Again, Tab. 22.1 lists examples of the contribution of the Lifshitz/Van der Waals contribution for commonly used testing liquids.

22.3.6 Zisman Extrapolation

American chemist William Zisman was one of the most important scientists in surface physics. He did a number of important experiments in surface characterization and invented a number of important techniques. One of these is the concept of the *critical surface tension* γ_c. From this concept the *Zisman extrapolation* arises.

Zisman observed that when plotting the cosine of the static contact angle $\cos\Theta$ of liquids with different surface tensions on the same solid, the values fall on a straight line [17]. This is true only for liquids that do not undergo strong hydrogen bonding, *i.e.*, for liquids with lower surface tension. By extrapolating this line to $\cos\Theta = 1$, *i.e.*, to a contact angle of $\Theta = 0$, one can find the critical surface tension. It is defined as the surface tension a liquid would need to have in order to be made completely wet on this surface.

The critical surface tension is an important technique for characterizing materials because it is, in contrast to the free surface energies, a material constant and does not depend on a second fluid. Fig. 22.7 shows an example of such a Zisman extrapolation on a polymer surface made from a perfluorinated polyether acrylate. The liquids used are water, ethanol, dichloromethane, ethylene glycol, acetophenone, and isopropanol for which the surface tensions are shown in Tab. 20.2. The calculated critical surface tension is around $\gamma_c \approx 12\,\mathrm{mN\,m^{-1}}$, which highlights one important property of polytetrafluoroethylene, of all fluorinated polymers: they have very low critical surface tensions (see Tab. 22.3). This means that in order for a liquid to spread on a fluorinated surface, the liquid must have a very low surface tension. Not many liquids fall into this category. The Zisman extrapolation is an exception to the techniques commonly used for characterizing the free energy of a surface. It does not account for the individual contributions of disperse, polar, or similar interactions to the overall surface

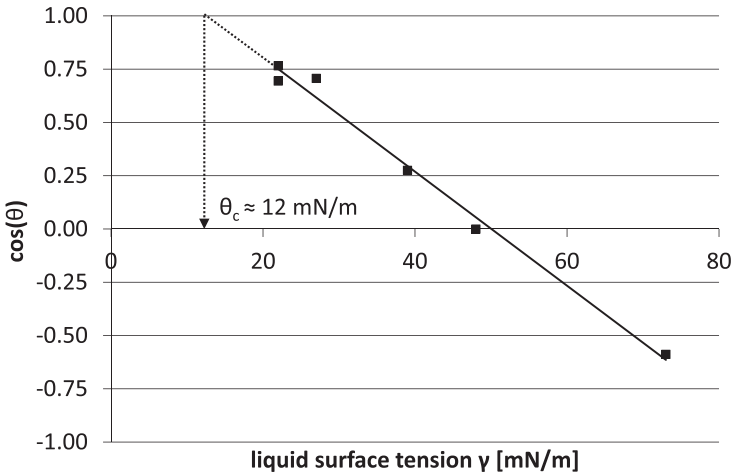

Fig. 22.7 *Example of a Zisman extrapolation on a perfluorinated polyether acrylate surface. The critical surface tension is determined to be* $\gamma_c \approx 12\,\mathrm{mN\,m^{-1}}$*, which is a very low value.*

Tab. 22.2 *Critical surface tension values of selected low free surface energy polymers. Taken from [18]*

Polymer	Repetition unit	Critical surface tension γ_c [mN m^{-1}]
Nylon 6,6	$-CO(CH_2)_4CONH(CH_2)_6NH-$	46
PVDC	$-CH_2-CCl_2-$	40
PVC	$-CH_2-CHCl-$	39
PVA	$-CH_2-CH(OH)-$	37
PS	$-CH_2-CH(C_6H_5)-$	33
PE	$-CH_2-CH_2-$	31
PCTFE	$-CF_2-CClF-$	31
PVF	$-CH_2-CHF-$	28
PVDF	$-CH_2-CF_2-$	25
PDMS	$-Si(CH_3)_2-O-$	24
PTFE	$-CF_2-CHF_2-$	22
PTFE	$-CF_2-CF_2-$	18.5
PHFP	$-CF_2-CF(CF_3)-$	16.2

Tab. 22.3 *Critical surface tension values of selected low free surface energy surfaces [18]*

Surface chemistry	Critical surface tension γ_c [mN m^{-1}]
Fluorocarbon surfaces	
$-CF_3$	6
$-CF_2H$	15
mixture of $-CF_3$ and $-CF_2-$	17
$-CF_2-CF_2-$	18
$-CF_2-CFH-$	22
$-CF_2-CH_2-$	25
$-CFH-CH_2-$	28
Hydrocarbon surfaces	
$-CH_3$	20-24
$-CH_2-CH_2-$	31
$-C_6H_5$ (aromatic)	35
Chlorocarbon surfaces	
$-CClH-CH_2-$	39
$-CCl_2-CH_2-$	40
$=CCl_2$	43

energy. It also does not measure the free surface energy but, as stated, the critical surface tension, which in most cases amounts to almost the same value. The Zisman extrapolation should be applied only if one predominant interaction is expected, *e.g.*, for the characterization of the wetting behavior of hydrocarbons on polymers which are both dominated by disperse forces. If this is not the case, the Zisman extrapolation tends to be inexact.

The Zisman extrapolation is the only relevant *one-component method*, as it does not measure the individual contributions to the free surface energy but assesses them as only one effect. As a result, all other techniques discussed so far are classified as *two-component methods* (if they account for two contributions, *e.g.*, polar and disperse) or as *multi-component methods* if they include more than two effects.

22.4 SUMMARY

In this section we studied methods that allow us to measure the surface tension of liquids. Several convenient methods allow quick and adequate determination of the surface tension. One of the more elaborate and industrially relevant methods is the *pendant drop analysis*, which we will study in section 24.5. In contrast to a liquid's surface tension, measuring the free surface energy of solids is less straightforward. As we have seen, several theories allow deriving the free energy of a surface from the characteristic contact angles that selected liquids will form on these surfaces. Depending on the chosen method, several liquids need to be tested. From the combined contact data of these liquids, the free surface energy can be determined. We have seen two examples of these methods using commonly encountered polymers.

REFERENCES

[1] P. L. du Noüy. "An interfacial tensiometer for universal use." In: *The Journal of General Physiology*, vol. 7, no. 5 (1925), pp. 625–631 (cit. on p. 453).

[2] L. Wilhelmy. "Ueber die Abhängigkeit der Capillaritäts-Constanten des Alkohols von Substanz und Gestalt des benetzten festen Körpers." In: *Annalen der Physik*, vol. 195, no. 6 (1863), pp. 177–217 (cit. on p. 453).

[3] T. Tate. "XXX. On the magnitude of a drop of liquid formed under different circumstances." In: *The London, Edinburgh, and Dublin Philosophical Magazine and Journal of Science*, vol. 27, no. 181 (1864), pp. 176–180 (cit. on p. 455).

[4] B. Vonnegut. "Rotating bubble method for the determination of surface and interfacial tensions." In: *Review of scientific instruments*, vol. 13, no. 1 (1942), pp. 6–9 (cit. on p. 457).

[5] F. M. Fowkes. "Attractive forces at interfaces." In: *Industrial & Engineering Chemistry*, vol. 56, no. 12 (1964), pp. 40–52 (cit. on p. 460).

[6] F. M. Fowkes. "Determination of interfacial tensions, contact angles, and dispersion forces in surfaces by assuming additivity of intermolecular interactions in surfaces." In: *The Journal of Physical Chemistry*, vol. 66, no. 2 (1962), pp. 382–382 (cit. on p. 460).

[7] C. J. Van Oss. *Interfacial forces in aqueous media*. CRC press, 2006 (cit. on p. 461).

[8] H. Erbil. *Solid and liquid interfaces*. Blackwell Publishing, Oxford, 2006 (cit. on p. 461).

[9] D. R. Lide. *CRC handbook of chemistry and physics*. 84th ed. CRC press, 2003 (cit. on p. 461).

[10] F. M. Fowkes. "Surface effects of anisotropic London dispersion forces in n-alkanes." In: *The Journal of Physical Chemistry*, vol. 84, no. 5 (1980), pp. 510–512 (cit. on p. 462).

[11] D. K. Owens and R. Wendt. "Estimation of the surface free energy of polymers." In: *Journal of Applied Polymer Science*, vol. 13, no. 8 (1969), pp. 1741–1747 (cit. on p. 462).

[12] W. Rabel. "Einige Aspekte der Benetzungstheorie und ihre Anwendung auf die Untersuchung und Veränderung der Oberflächeneigenschaften von Polymeren." In: *Farbe und Lack*, vol. 77, no. 10 (1971), pp. 997–1006 (cit. on p. 462).

[13] D. Kaelble. "Dispersion-polar surface tension properties of organic solids." In: *The Journal of Adhesion* (1970) (cit. on p. 462).

[14] S. Wu. "Calculation of interfacial tension in polymer systems." In: *Journal of Polymer Science Part C: Polymer Symposia*. Vol. 34. 1. Wiley Online Library. 1971, pp. 19–30 (cit. on p. 462).

[15] S. Wu. "Polar and nonpolar interactions in adhesion." In: *The Journal of Adhesion*, vol. 5, no. 1 (1973), pp. 39–55 (cit. on p. 462).

[16] C. J. Van Oss, M. K. Chaudhury, and R. J. Good. "Interfacial Lifshitz-van der Waals and polar interactions in macroscopic systems." In: *Chemical Reviews*, vol. 88, no. 6 (1988), pp. 927–941 (cit. on p. 463).

[17] E. G. Shafrin and W. A. Zisman. "Constitutive relations in the wetting of low energy surfaces and the theory of the retraction method of preparing monolayers." In: *The Journal of Physical Chemistry*, vol. 64, no. 5 (1960), pp. 519–524 (cit. on p. 463).

[18] Zisman and Jarvis. *Surface Chemistry of Fluorochemicals*. Report. Naval Research Lab Washington, 1965 (cit. on p. 464).